



Sensitivity analysis of low-velocity impact response of laminated plates



G.O. Antoine, R.C. Batra*

Department of Biomedical Engineering and Mechanics, M/C 0219, Virginia Polytechnic Institute and State University, Blacksburg, VA 24061, USA

ARTICLE INFO

Article history:

Received 4 September 2014
Received in revised form
1 December 2014
Accepted 4 December 2014
Available online 12 December 2014

Keywords:

Sensitivity analysis
Analysis of variance
Correlation coefficients

ABSTRACT

We analyze the sensitivity to values of material parameters, layer thickness and impact speed of the plate deflection, the contact force between the impactor and the plate, the maximum length of a crack, and the energy dissipated during the low velocity impact at normal incidence of a clamped rectangular laminate by a rigid hemispherical-nosed cylinder. The laminate is comprised of layers of polymethylmethacrylate (PMMA) and polycarbonate (PC) bonded by an adhesive, and its deformations are analyzed by the finite element method. The mathematical and computational models of the system have been described in our previous work, and their predictions compared with test data (*Composite Structures*, 116, 193–210, 2014). The thermo-elasto-viscoplastic materials of the PMMA and the PC and the viscoelastic material of the adhesive involve a large number of material parameters whose precise values are unknown. Here we consider values of eleven material parameters – five for the PMMA, five for the PC and one for the adhesive. It is found that values of Young's moduli and Poisson's ratios of the PMMA and the PC, and the shear modulus of the adhesive strongly influence the plate deflection and the crack length. Values of material parameters of the PC that noticeably affect its plastic deformations also determine the energy dissipation whose correlation with the second peak in the contact force between the impactor and the laminate is exhibited. The PMMA layer thickness is found to influence the crack length and the PC layer thickness the energy dissipated.

© 2014 Elsevier Ltd. All rights reserved.

1. Introduction

Mathematical models of engineering structures generally involve a system of either ordinary or partial differential equations whose coefficients depend upon values of numerous material parameters. For a fixed set of initial and boundary conditions, the structural response depends upon materials of structural components. A goal of sensitivity analysis is to explore the effect on the structural response of variability or uncertainty in the knowledge of values of material and geometric parameters of the structure.

While studying the response of glass targets to hypervelocity impact by small impactors, Anderson and Holmquist [1,2] analyzed the sensitivity of the computed results to small variations in the impact speed. They considered impact velocities of 2238, 2238.0001, 2238.0002, 2066 and 2066.0001 m/s, and found that a small variation in the impact speed noticeably affected the propagation of the penetration and failure fronts. In particular, the final

depth of the failure and the penetration fronts increased by about 20% and more than 10%, respectively, with a 0.0001 m/s or 5×10^{-5} % increase in the impact velocity, showing the high sensitivity of their computational model upon the impact speed. Poteet and Blosser [3] used sensitivity analysis to find the design factor with the greatest effect in the hypervelocity impact resistance of a bumper metallic protection system comprised of three metallic layers with spacing between them. Taking the layer thickness and the spacing between two adjacent layers as design variables, and the damage to the substructure and the debris dispersion as measures of the structure performance, the parameters with the largest effect on structure's integrity were found to be the thickness of the first layer and the spacing between the layers.

Here we determine material and geometric parameters that significantly affect the laminate deflection, the energy dissipated, the contact force between the impactor and the laminate, and lengths of cracks, if any, formed in a layer. The laminate comprised of polymethylmethacrylate (PMMA)/adhesive/polycarbonate (PC) is impacted at normal incidence by a low-velocity smooth hemispherical-nosed rigid cylinder. The constitutive equations used to model the thermoviscoplastic response of the PMMA and

* Corresponding author. Tel.: +1 540 231 6051; fax: +1 540 231 4574.

E-mail addresses: antoineg@vt.edu (G.O. Antoine), rbatra@vt.edu (R.C. Batra).

the PC involve 30 material parameters whose values cannot be precisely determined. Here we first screen values of material parameters to find 5 material parameters each for the PMMA and the PC that significantly affect the system response. Subsequently, we use the sampling-based sensitivity method to ascertain the influence of these parameters on the system response by considering either 10% or 30% variation in the values of these parameters. We note that the uncertainty in the values of material parameters is *a priori* unknown and requires data from numerous experiments performed under controlled conditions. In the absence of this data, the assumed 30% variability in the values of material parameters is probably an upper limit.

The rest of the paper is organized as follows. We briefly describe the impact problem studied in Section 2 and provide a comparison of the computed and the test results. The screening method and the selection of five important material parameters for the PMMA and the PC are discussed in Section 3. The details of the sensitivity analysis for the impact problem are given in Section 4, and conclusions of the work are summarized in Section 5.

2. Problem description

2.1. Initial-boundary-value problem

We perform sensitivity analysis of the impact problem schematically sketched in Fig. 1 and described in Antoine and Batra [4]. The smooth hemispherical nosed rigid impactor of mass 28.5 g and 6.9 J initial kinetic energy impacts at normal incidence a clamped flat $L_1 \times L_2 \times h$ ($h = h_1 + h_2 + h_3$) rectangular plate. We refer the reader to [4] for details of the analysis of deformations of the laminate by the finite element method (FEM) using the commercial FE software, LS-DYNA, in which material models for the PC, the

PMMA and the adhesive have been implemented as user defined subroutines. The convergence of results with the refinement of the FE mesh and other details of the computational work (e.g., energy of hour-glass control algorithms) are described in Ref. [4]. In the present analysis a fixed FE mesh comprised of 8-node brick elements has been employed, and deformations of only a quarter of the laminate have been analyzed due to the symmetry of the problem geometry, and initial and boundary conditions. This FE mesh gave a converged solution of the impact problem, e.g., see Ref. [4]. Results have been computed for $L_1 = L_2 = 127$ mm, $h_1 = h_3 = 1.5875$ mm and $h_2 = 0.635$ mm.

2.2. Validation of the model

For the sake of completeness we describe below a few salient features of the model and give some results.

Constitutive equations proposed by Mulliken and Boyce [5] and modified by Varghese and Batra [6] used to model the PMMA and the PC materials are given in the Appendix. Values of the material parameters and methods to find them can be found in Refs. [5–7]. These references also show that the predicted and the experimental stress-strain curves for the PMMA and the PC deformed in uniaxial compression compare well with each other from at low and high strain rates thereby establishing the appropriateness of their values and the material model.

The failure criteria for the PMMA and the PC adopted from the literature are given in Ref. [4]. The brittle failure of the PMMA is modeled using a maximum threshold for the principal stresses (Fleck et al. [8]), and its ductile failure is assumed to occur when the accumulated equivalent plastic strain reaches 5% (Stickle and Schultz [9]). The PC is assumed to have only ductile failure when the maximum effective plastic strain at a point equals 3 (similar to

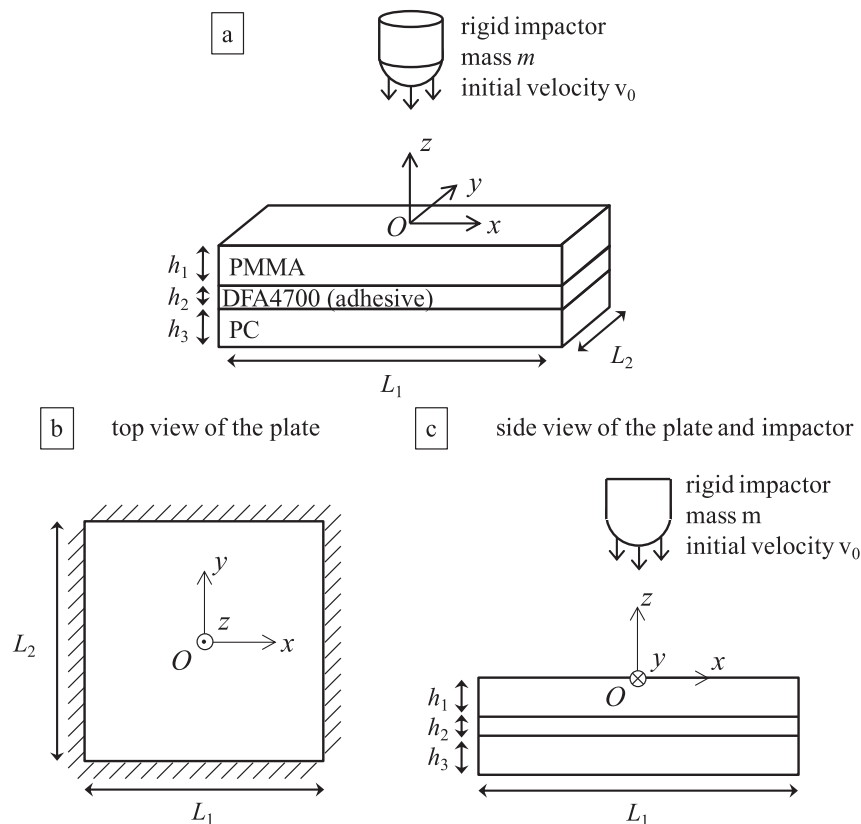


Fig. 1. Schematic sketch of the impact problem studied.

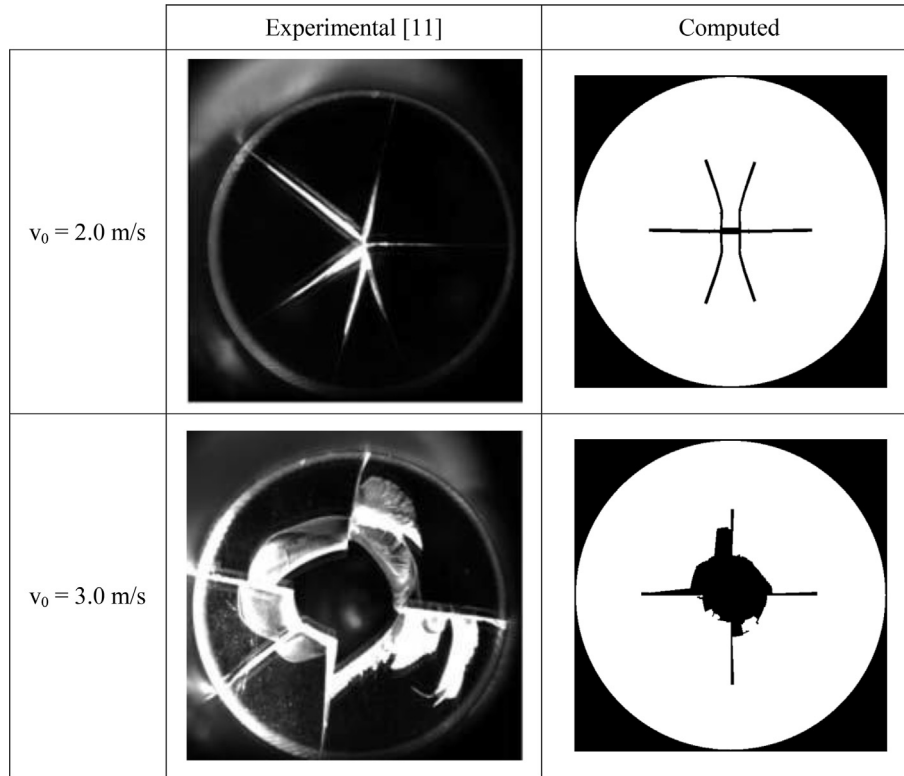


Fig. 2. Experimental and computed fracture patterns in the PMMA panels impacted at normal incidence by the rigid cylindrical impactor translating at 2.0 and 3.0 m/s; from [4].

Richards et al. [10] who used 2 as plastic strain at failure). Failed elements are deleted from the analysis domain.

For the test configurations employed by Zhang et al. [11] (i.e., clamped 6.35 mm thick and 76.2 mm diameter PMMA plates impacted at about 3 m/s by a 6.95 kg cylindrical impactor with hemispherical nose of 12.7 mm diameter) the experimental and the computed fracture patterns are compared in Fig. 2 for two impact velocities. It is clear that the two sets of results agree well, validating the mathematical model for the PMMA plates.

For the impact tests on clamped square PC plates of 254 cm edge length but of varying thickness impacted by 104 g hemispherical nosed 12.7 cm diameter steel cylinders conducted by Gunnarsson et al. [12] at impact velocities between 10 m/s and 50 m/s, we have compared in Table 1 the maximum deflection measured at the center of the rear face of the PC plates. The maximum difference in the two sets of values of 10.3% validates the mathematical and the

computational model for the impact of the PC plate, at least for finding the maximum deflections.

The DFA4700 adhesive is modeled as a nearly incompressible nonlinear viscoelastic material with the quasi-static elastic response given by Ogden's [13] strain energy density and the strain-rate dependent response by Prony series (Christensen [14]). Experimental stress-strain curves for uniaxial tensile tests of DFA4700 deformed at different engineering strain rates are compared to their model predictions in Fig. 3. Note that the maximum logarithmic strain of 0.69 corresponds to 100% engineering strain. There is less than 10% average deviation between the experimental and numerical stress-strain curves. Details of determining values of material parameters from the test data are given in Ref. [22].

Delamination at interfaces between two materials is simulated by using a traction-separation law implemented in LSDYNA. Values

Table 1
Comparison of the experimental and the computed maximum deflections (measured at the center of the back face of the plate) of the clamped circular PC panels; from [4].

Panel thickness [mm]	Impact velocity [m/s]				
	10	20	30	40	50
	Experimental (computed) maximum deflection [mm]				
3.00	13.2 (13.0) error: -1.5%	16.1 (17.1) error: +6.2%			
4.45	9.4 (9.0) error: -4.3%	12.9 (13.1) error: +1.6%			
5.85	6.5 (7.1) error: +9.2%	10.9 (10.2) error: -6.4%	15.2 (14.8) error: -2.6%	19.2 (19.0) error: -1.0%	22.0 (22.7) error: +3.2%
9.27			10.2 (10.4) error: +2.0%	11.3 (12.1) error: +7.1%	14.0 (14.8) error: +5.7%
12.32			6.9 (7.3) error: +5.8%	8.7 (9.6) error: +10.3%	10.7 (11.3) error: +5.6%

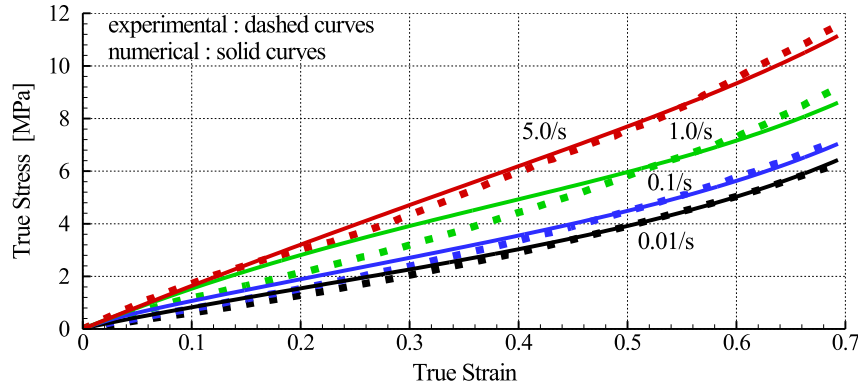


Fig. 3. Experimental and numerical results for the uniaxial tensile deformations of DFA4700 at different engineering strain rates; from [4].

of the critical energy release rates and of the separations at failure for modes I and II are given in Ref. [4].

Simulation results for impacts at 12 m/s and 22 m/s of clamped PMMA/DFA4700/PC laminates are compared with the experimental findings of Stenzler [15,16] in Fig. 4, Fig. 5 and Table 2. It is obvious that the two sets of results are close to each other, which implies that the mathematical model and its implementation in LS-DYNA capture well the response of the laminate. A possible explanation for the large difference in the computed and experimental values of the first peak in the reaction force is given in Ref. [22].

3. Screening of variables

3.1. Purpose of screening

The constitutive equations for the PMMA and the PC have 15 material parameters each giving a total of 30 parameters. To reduce the number of variables for the sensitivity analysis it is expedient to identify a small subset of material parameters that are likely to have a large influence on the mechanical response of the materials, and hence on the impact response of the laminate. This can be accomplished by a screening analysis that gives qualitative indicators to rank the input parameters (e.g., values of the material parameters) in order of their importance for the variability of the output (here the stress-strain response of the material). The method used to identify the subset of important parameters is presented in the next paragraph. Then it is applied to find parameters for the PMMA and the PC that significantly affect their response to mechanical deformations.

3.2. Description of the method

We use the global one-factor-at-a-time (OAT) screening method proposed by Morris [17], and illustrate it by considering a scalar-valued (response) function y of k input variables x_1 through x_k that have been normalized to take real values between 0 and 1. For the screening analysis we require the input factors to take values in the set $\{0, 1/(p-1), \dots, 1\}$ where p is an integer. With the definition $\Delta = p/(2(p-1))$ the elementary effect of the i th factor at the point $\mathbf{x} = (x_1, \dots, x_k)$ is

$$d_i(\mathbf{x}) = \frac{1}{\Delta} [y(x_1, \dots, x_{i-1}, x_i + \Delta, x_{i+1}, \dots, x_k) - y(x_1, \dots, x_k)] \quad (1)$$

The number $d_i(\mathbf{x})$ measures the sensitivity of the response function with respect to the i th input factor at the point \mathbf{x} , and can be interpreted as an approximation to the partial derivative of y with respect to x_i . Following Saltelli et al. [18], we choose an even integer p and then use the following procedure to compute

elementary effects of all input factors. In Morris's method the impact of each input factor is evaluated in turn.

First, a base vector \mathbf{x}^* is chosen whose components are randomly taken from the set $\{0, 1/(p-1), \dots, 1-\Delta\}$. A subset χ of the set $\{1, 2, \dots, k\}$ is then randomly chosen, and the vector $\mathbf{x}^{(1)} = (x_1^{(1)}, \dots, x_k^{(1)})$ is formed according to the following rule:

$$x_i^{(1)} = \begin{cases} x_i^* + \Delta & \text{if } i \in \chi, \\ x_i^* & \text{otherwise.} \end{cases} \quad (2)$$

The successive vectors $\mathbf{x}^{(1)}, \dots, \mathbf{x}^{(k+1)}$ are computed as follows. Assuming that the vector $\mathbf{x}^{(n)}$ ($n \leq k$) is known, an index i such that the i th component of the input has not been changed yet (i.e., $\forall m \leq n, x_i^{(m)} = x_i^{(1)}$) is randomly selected and the vector $\mathbf{x}^{(n+1)}$ is defined as

$$x_i^{(n+1)} = \begin{cases} x_i^{(n)} - \Delta & \text{if } i \in \chi, \\ x_i^{(n)} + \Delta & \text{otherwise.} \end{cases} \quad (3)$$

The estimated elementary effect, \tilde{d}_i , of the factor i for the base vector \mathbf{x}^* is then given by

$$\tilde{d}_i = \begin{cases} \frac{1}{\Delta} [y(\mathbf{x}^{(n)}) - y(\mathbf{x}^{(n+1)})] & \text{if } i \in \chi, \\ \frac{1}{\Delta} [y(\mathbf{x}^{(n+1)}) - y(\mathbf{x}^{(n)})] & \text{otherwise.} \end{cases} \quad (4)$$

A compact way to write and implement the procedure described above is the following. Define the orientation matrix \mathbf{B}^* as the matrix whose rows are the $\mathbf{x}^{(n)}$'s, $1 \leq n \leq k+1$. That is,

$$\mathbf{B}^* = \left(\mathbf{J}_{k+1,1} \mathbf{x}^* + \frac{\Delta}{2} [(2\mathbf{T}_{k+1,k} - \mathbf{J}_{k+1,k}) \mathbf{D}^* + \mathbf{J}_{k+1,k}] \right) \mathbf{P}^* \quad (5)$$

where $\mathbf{J}_{k+1,1}$ is the $(k+1) \times k$ matrix whose entries are all equal to 1, \mathbf{x}^* is the $1 \times k$ row base vector, $\mathbf{T}_{k+1,k}$ is the $(k+1) \times k$ strictly lower triangular matrix of 1's, \mathbf{D}^* is a diagonal matrix with elements randomly chosen from the set $\{-1, +1\}$, and \mathbf{P}^* is a random $k \times k$ permutation matrix. The response function y is evaluated by taking the rows of \mathbf{B}^* as successive input points, and the elementary factors are calculated.

This provides one value of \tilde{d}_i since each input factor is changed once. Repeating the procedure r times (r is an integer) with r random values for the base vector \mathbf{x}^* and randomly selecting each time a new χ provides r independent measures of \tilde{d}_i . Since these values are independent one can compute their mean and standard deviation. The large mean values indicate factors that significantly affect the output. Thus mean values of \tilde{d}_i rank the input factors

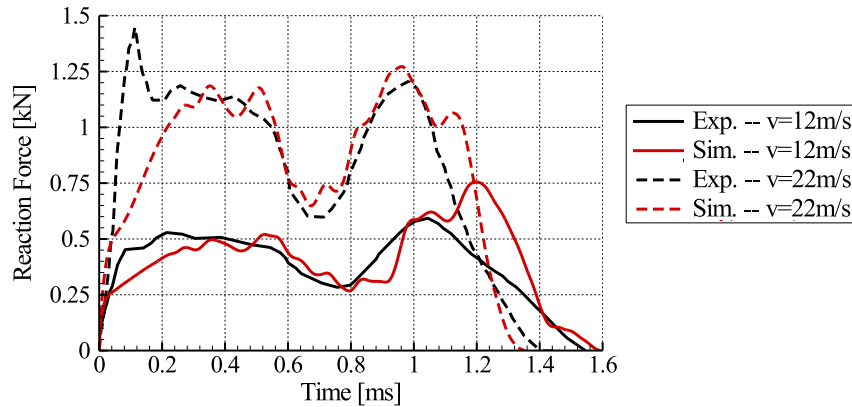


Fig. 4. Experimental (dark curves) and computed (red curves) reaction force time histories for the PMMA/DFA4700/PC plate impacted at 12 m/s (solid curves) and 22 m/s (dashed curves); from [4]. (For interpretation of the references to colour in this figure legend, the reader is referred to the web version of this article.)

according to their importance in the output variability. High values for the standard deviations indicate factors that have strong interactions with other inputs.

3.3. Results

The material parameters, x_i 's, for the PMMA and the PC are $\dot{\gamma}_{0,\alpha}^p$, ΔG_α , α_α^p , h_α , t_α^{ss} , $\dot{\gamma}_{0,\beta}^p$, ΔG_β , α_β^p , h_β , t_β^{ss} , C_R , N_I , c , ν , E (see Appendix I (or Mulliken and Boyce [5] and Varghese and Batra [6]) for their definitions). The components of the input vector \mathbf{x} are values of the normalized material parameters \hat{x}_i defined as

$$\hat{x}_i = \frac{x_i - \alpha_{\min}}{\alpha_{\max} - \alpha_{\min}} \quad (6)$$

For normalizing the x_i 's we use their nominal values x_i^0 (given in Appendix I, [5] and [6]), and assume that $\alpha_{\min} = 0.7$, $\alpha_{\max} = 1.3$. The normalized parameters \hat{x}_i are allowed to vary between 0 and 1, corresponding to $\pm 30\%$ variation of the input factors about their respective nominal values. This implies that the assumed range of uncertainty in values of material parameters is 30%. As noted earlier, this is probably an upper limit on the variability of values of material parameters.

We use as response function y the stress-strain curve of the PMMA and the PC for uniaxial compression deformation at strain rate of 5000/s up to -0.2 true axial strain. Since this is not a scalar-valued function, we replace $y(\mathbf{x}^{(n+1)}) - y(\mathbf{x}^{(n)})$ in Eq. (4) by

$$\sqrt{\int_{\varepsilon=0}^{0.2} (\sigma(\mathbf{x}^{(n+1)}, -\varepsilon) - \sigma(\mathbf{x}^{(n)}, -\varepsilon))^2 d\varepsilon}$$

where $\sigma(\mathbf{x}, \varepsilon)$ is the true axial stress for true axial strain ε and values of material parameters corresponding to point \mathbf{x} .

For the present study we set $r = 8$ and compare results obtained with $p = 4$ and $p = 12$. Therefore 128 stress-strain curves are necessary for each value of p and each material for a total of 512 simulations. The mean and the standard deviations of the elementary effects, \hat{d}_i , are depicted in Fig. 6.

We have indicated in Fig. 6 the variables whose elementary effects are clearly separated from the group of points with low mean and low standard deviations. We notice that results obtained with $p = 4$ and 12 are qualitatively similar, and in particular the five material parameters with the highest mean effects are E , ν , ΔG_α , α_β^p , t_β^{ss} for the PMMA and E , ν , ΔG_α , t_α^{ss} , ΔG_β for the PC. We conduct the sensitivity analysis of the impact problem described in Section 2 with respect to these material parameters.

4. Sensitivity analysis of the impact problem

4.1. Method

4.1.1. Input factors for material parameters

Because of the presence of more than one shear modulus in the constitutive relation for the adhesive, for the sensitivity analysis we assume that all shear moduli, μ_n and G_m , are multiplied by the same

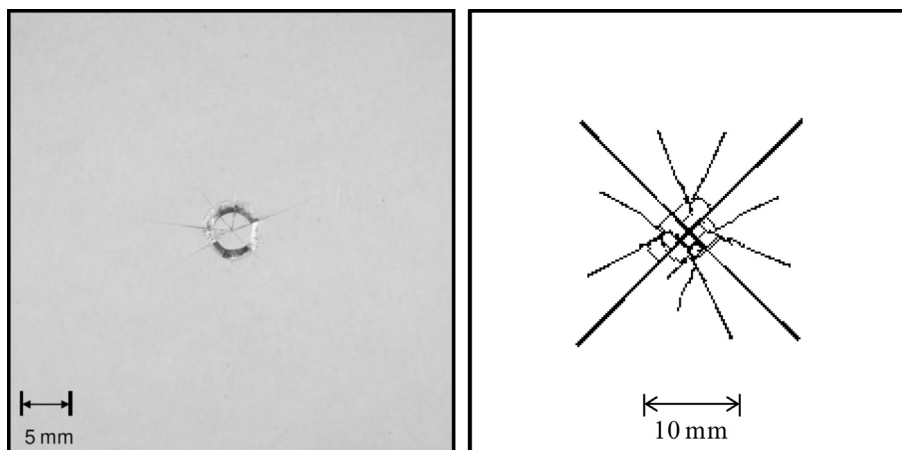


Fig. 5. Details of the experimental [15] (left) and the computed (right) fracture pattern on the back surface of the PMMA plate of the PMMA/DFA4700/PC laminate for the impact speed of 22 m/s; from [4].

Table 2

Comparison of the experimental and the computed fracture patterns on the back surface of the PMMA plate for the PMMA/DFA4700/PC laminate; from [4].

Impact velocity [m/s]	Experimental	Computed
12	No damaged material at the impact site 5 cracks, length 4–7 mm	No damaged material at the impact site 4 cracks, length 10–11 mm
22	Diameter of damaged zone at the impact site = 5 mm 7 cracks, length 11–12 mm	Diameter of damaged zone at the impact site = 6 mm 8–9 cracks, length 10–11 mm

scaling factor while exponents, α_n , of the stretches in the expression for the Ogden strain energy density and the decay constants β_m (inverse of relaxation times) of the Prony series are left unchanged. Consequently the instantaneous shear modulus G_0 of the modified material is different from that of the original material. The initial Poisson's ratio of the adhesive is set to 0.498 and is unchanged during the sensitivity study. With 5 material parameters for the PMMA, 5 for the PC and 1 for the DFA4700 listed in Table 3, there are 11 material parameters (or input factors) for the sensitivity study.

The material parameters are normalized with respect to their nominal values (see Eq. (6)) either with $\alpha_{\min} = 0.7$, $\alpha_{\max} = 1.3$ or with $\alpha_{\min} = 0.9$, $\alpha_{\max} = 1.1$. The normalized variables vary between 0 and 1 leading to either 30% or 10% variation about their nominal values.

4.1.2. Input factors for the geometric parameters and the impact velocity

The input factors are the thicknesses h_1 , h_2 and h_3 , of the three layers and the impact velocity v_0 . The manufacturer of the PMMA and the PC layers gives ± 0.0762 mm uncertainty in the layer thickness. Assuming that the uncertainty in the adhesive layer

Table 3

Material parameters included for the sensitivity study of the impact problem.

Material	Parameters selected for the sensitivity study
PMMA	$E, \nu, \Delta G_\alpha, \alpha_\beta^p, t_\beta^{ss}$
PC	$E, \nu, \Delta G_\alpha, t_\alpha^{ss}, \Delta G_\beta$
Adhesive	$G_0 \left(= \sum_{n=1}^N \frac{1}{2} \mu_n \alpha_n + \sum_{m=1}^M G_m \right)$

thickness is also ± 0.0762 mm the three thicknesses are allowed ± 0.0762 mm variation with uniform probability. In the list of impact velocities reported by Stenzler [15] the experimental v_0 ranges between 21 m/s and 23 m/s, therefore 1 m/s uncertainty with uniform probability in the impact velocity about the nominal value 22 m/s is assumed.

4.1.3. Description of the method

To investigate the effect of uncertainty in the inputs (e.g., the material parameters) on the output (the plate response) we use a sampling-based method, which has been shown to be robust with relatively small samples (~200) [19,20]. It estimates the uncertainty in the output generated by uncertainty in the inputs, and assesses the importance of the individual input factors on the uncertainty in the results. More specifically, results considered are the post-impact length of cracks formed in the PMMA layer, the total energy dissipated in the laminate, the history of the contact force between the impactor and the laminate, and the deflection of the laminate.

We use the Latin-hypercube sampling method to generate different inputs. The normalized input \hat{x}_k , given by Eq. (6), varies between 0 and 1 with an assumed uniform distribution. The corresponding cumulative probability is $f(\hat{x}) = \hat{x}$ if $0 \leq \hat{x} \leq 1$. Assuming that the input factors are not correlated, the Latin-hypercube sampling method can be performed in a simple way. First, the number of samples is chosen. We use here 300 samples, which is large enough to limit the correlation of the 11 input variables and small enough to be computationally reasonable since only 300 impact simulations are required. Then, the interval $[0, 1]$ is partitioned into 300 segments $[a_{j-1}, a_j]$, $a_j = (j-1)/300$, $j = 1, \dots, 300$ of equal size. The values $b_j = f^{-1}(a_j)$ are then determined and a random value $\hat{x}_k^{(j)}$ is selected in each of the $[b_{j-1}, b_j]$ intervals for the k th normalized input factor \hat{x}_k . The procedure is repeated independently for each of the 11 input variables, giving a list of 300 values for each input. The values are then randomly paired to form 300 samples, i.e., a set of 300 vectors of length 11. The impact problem is then analyzed for each of the 300 sets of values for the material parameters with 10% ($\alpha_{\min} = 0.9$, $\alpha_{\max} = 1.1$) and 30% ($\alpha_{\min} = 0.7$, $\alpha_{\max} = 1.3$) uncertainty in the values of material parameters. Since it is easier to determine values of the elastic parameters for the PMMA and the PC than those of the remaining material parameters both studies described above are also carried out with Young's moduli and Poisson's ratios of the PMMA and the PC set to their nominal values. In the latter cases the 7 remaining inputs are varied. Thus four studies (comprising 300 simulations each) are performed for a total of 1200 simulations. The sensitivity study with respect to the layer thickness and the impact velocity is carried out with 100 additional simulations.

4.2. Results

4.2.1. Distribution of the results for variations in values of material parameters

The distribution of results is shown in the box plots of Fig. 7 wherein the convention used for the box plots is also given.

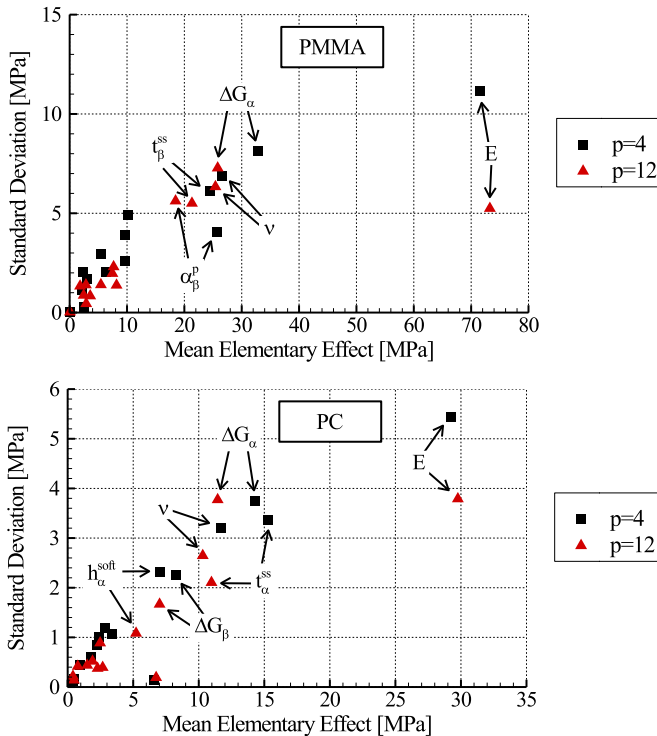


Fig. 6. The standard deviation vs. the mean elementary effect for the uniaxial compression of PMMA and PC at 5000/s true strain rate.

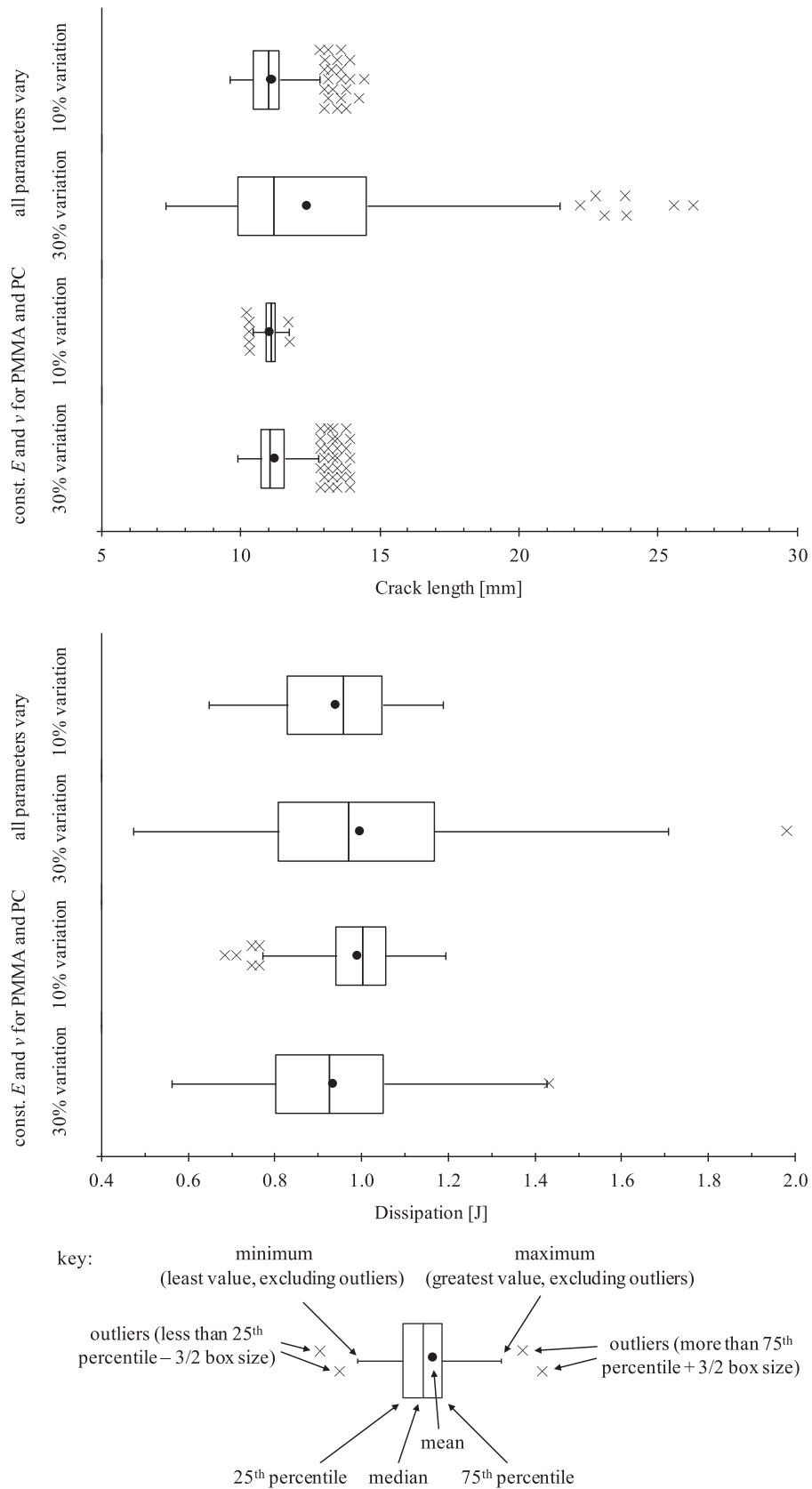


Fig. 7. Box plots of the energy dissipation and the post-impact crack length for 10 and 30% variations in values of input parameters with and without varying Young's moduli and Poisson's ratios of the PMMA and the PC.

The distribution shown in the box plots is consistent with the expectation that the scatter in the data is more important when the material parameters are varied over a larger range. In particular we note that when the elastic properties of the PMMA and the PC are fixed and 10% variation in values of the remaining four material parameters is allowed the scatter in the crack length is small (10.2 vs. 11.8 mm) while it is large when values of all parameters are allowed to vary by 30% (7.3 vs. 26.4 mm) since there is a factor of 3.6 between the largest and the smallest observations in the latter case. For the energy dissipation the scatter is considerable even with 10% variation in values of all parameters except for E and ν of the PMMA and the PC (0.69 vs. 1.19 J, ratio = 1.7). It is not surprising that with fixed values of E and ν for the PMMA and the PC the variability in the crack length is much smaller than that in the energy dissipation. The brittle failure of the PMMA is mostly affected by its Young's modulus while the main source of energy dissipation is plastic deformations of the PC which are affected by values of three parameters ΔG_{α} , t_{α}^{SS} and ΔG_{β} .

In Fig. 8 we have displayed time histories of the min, 10th, 50th (median), 90th percentiles, the max and the mean values of the contact force. These values are determined as follows: for each value of time the reaction forces obtained from different samples are collected and their percentiles and means are determined. Thus the curve corresponding to, for example, the minimum value of the contact force does not necessarily correspond to the contact force of the same sample throughout the entire impact duration.

In order to quantify the scatter in the contact force, the L^2 -norm of the contact force is computed for each set of input values. The computed difference between the mean and the max values of the L^2 -norm, and that between the mean and the min values of the L^2 -norm are listed in Table 4. Similar results for the deflection of the centroid of the bottom surface of the laminate are presented in Fig. 9 and Table 4.

Table 4

Differences between the min and the max values of the L^2 -norms of the reaction force and the maximum laminate deflection for 10% and 30% uncertainties in values of the input variables (taking the mean force/deflection as the reference).

	Reaction force		Deflection	
	Difference between min and mean	Difference between max and mean	Difference between min and mean	Difference between max and mean
±10% variation in all inputs	15.1%	13.9%	10.4%	7.33%
±30% variation in all inputs	30.2%	32.8%	33.1%	24.1%
±10% variation, constant E and ν for PMMA and PC	9.06%	8.64%	5.89%	4.58%
±30% variation, constant E and ν for PMMA and PC	14.4%	14.6%	11.9%	10.4%

For the 10% (30%) uncertainty in the input variables, the mean differs from the min and the max values of the deflection by about 10% (33%). For the reaction force the corresponding values are 15% (33%). However, when E and ν for the PMMA and the PC are not varied, then the maximum difference between the mean and the min/max values of the deflection and the reaction force are less than 15%. Thus the uncertainty in the values of the reaction force and the maximum deflection is about the same as that in the values of the input variables considered. It may be interpreted as follows: the output of these two variables continuously depends upon the input values of the material parameters.

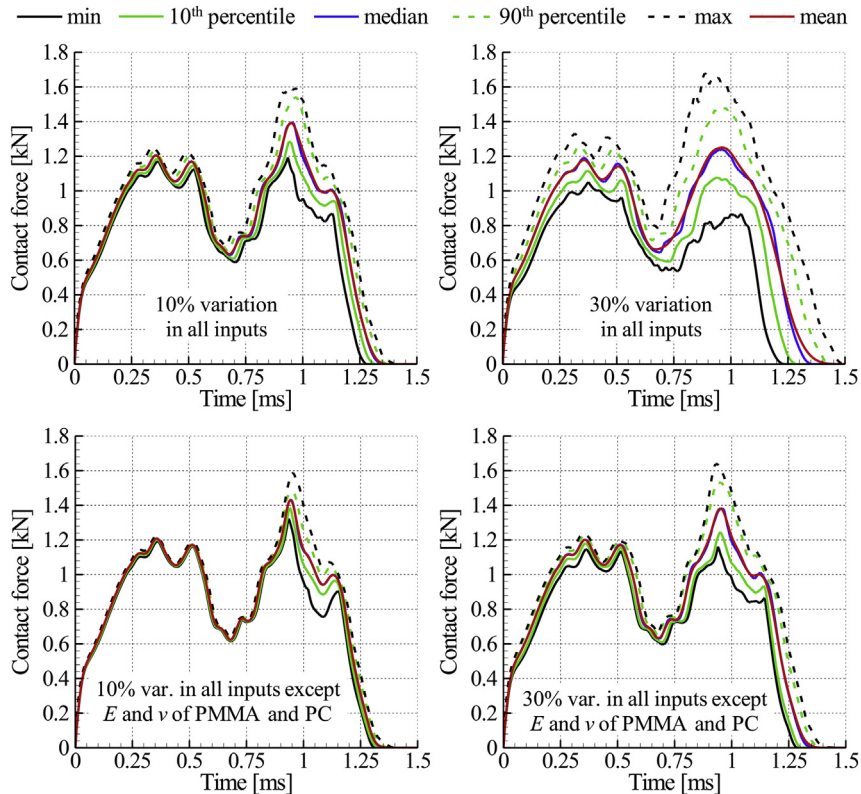


Fig. 8. Time histories of the minimum, 10th, 50th and 90th percentiles and the mean of the contact force.

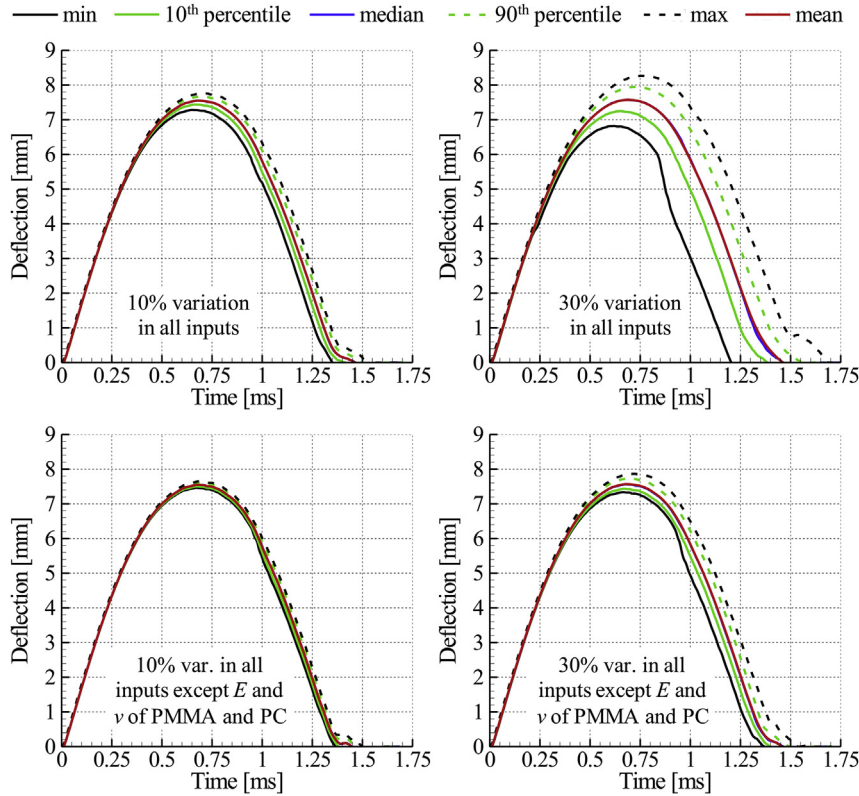


Fig. 9. Time histories of the minimum, 10th, 50th and 90th percentiles, and the mean of the deflection of the centroid of the bottom surface of the laminate.

It can be concluded from results presented in Table 4 that the experimentally measurable outputs such as the crack length, the reaction force, and the laminate deflection show less scatter than the energy dissipation which cannot be measured in physical tests. Therefore it is possible that the computed energy dissipation is far from the actual one even when the mathematical model has been validated by ensuring that the experimentally measurable outputs agree well with the computed ones. We also note that for the reaction force time history there is more scatter in values of the second peak than that in values of the first peak and of the “valley” defined as the value of the local minimum occurring at about 0.7 ms.

4.2.2. Distribution of results for variations in values of geometric parameters and impact velocity

The distribution of results of the impact simulations for variations in values of geometric parameters and impact velocity are shown in the box plots of Fig. 10.

Fig. 11 displays the min, the 10th, the 50th (median), the 90th percentiles, the max and the mean of the values of the contact force and the deflection as a function of time.

In order to quantify the scatter in the contact forces the average deviations (L^2 -norm) between the mean and the max values, and those between the mean and the min values are given in Table 5.

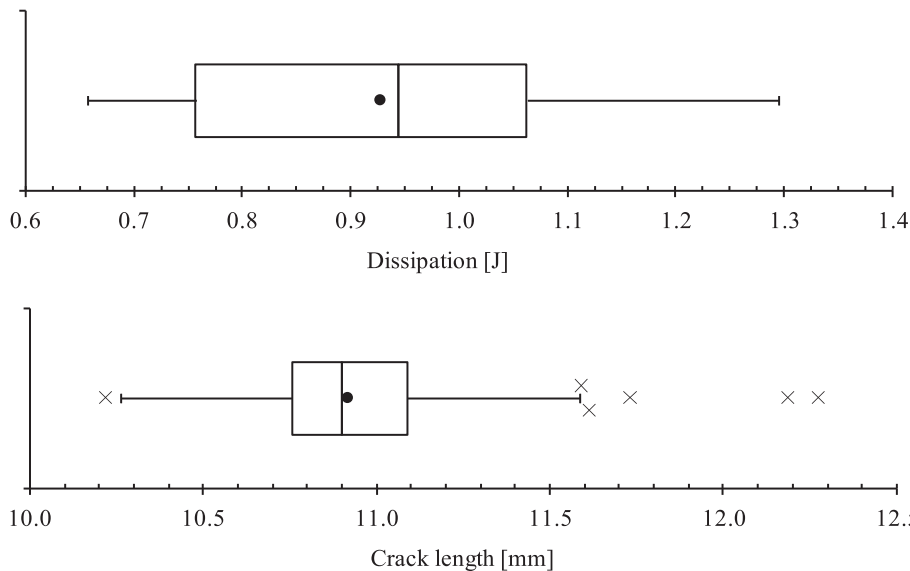


Fig. 10. Box plots of the energy dissipation and the post-impact crack length for variations in the geometric parameters.

4.2.3. Sensitivity analysis and correlation

Correlation is an important measure of characterizing the effect of input factors (i.e., material parameters) on the outputs (i.e., simulation results). The correlation r between two variables ξ_1 and ξ_2 is defined as

$$r = \frac{\sum_{i=1}^n (\xi_1^{(i)} - \bar{\xi}_1)(\xi_2^{(i)} - \bar{\xi}_2)}{\sqrt{\sum_{i=1}^n (\xi_1^{(i)} - \bar{\xi}_1)^2} \sqrt{\sum_{i=1}^n (\xi_2^{(i)} - \bar{\xi}_2)^2}} \quad (7)$$

where n is the total number of observations, $\xi_1^{(i)}$ and $\xi_2^{(i)}$ are values of variables corresponding to the i th observation, and $\bar{\xi}_1$ and $\bar{\xi}_2$ are mean values of variables ξ_1 and ξ_2 over the n observations, respectively. Because of the inner product inequality, the value of r is in the interval $[-1, 1]$ and describes simultaneous variations of the variables. For instance r is positive when ξ_1 and ξ_2 vary “in the same manner” [21]. Eq. (7) can be used to compute the correlation between the inputs and the outputs, and correlations among the input factors. In the present work, since the inputs are assumed to be independent of each other, it is important that their correlations be small, since otherwise output results will have no significance. The computed maximum magnitudes of the correlation among the inputs of 0.089 for variations of the material parameters and 0.05 for the other study (e.g., see Tables given in the Appendix) are indeed small.

The sensitivity coefficients quantify the effect of varying an input factor on the output. In order to find these we assume that the output y follows the relation

$$y_{\text{model}} = b_0 + \sum_{j=1}^m b_j \hat{x}_j \quad (8)$$

The output may not exactly follow relation (8), therefore, we write the observations $y^{(i)}$, $i = 1 \dots n$, as

$$y^{(i)} = b_0 + \sum_{j=1}^m b_j \hat{x}_j^{(i)} + \varepsilon^{(i)} \quad (9)$$

where $\varepsilon^{(1)} \dots \varepsilon^{(n)}$ are errors. Values of coefficients \mathbf{b} minimizing $\|\varepsilon\|_2$ are called the sensitivity coefficients. The quantity, R^2 , defined by

$$R^2 = \frac{\sum_{i=1}^n (y_{\text{model}}^{(i)} - \bar{y})^2}{\sum_{i=1}^n (y^{(i)} - \bar{y})^2} \quad (10)$$

Table 5

Average L^2 -norm deviations between the mean contact force and the minimum and the maximum forces (taking the mean force as reference) for variations in values of the plate thickness.

Reaction force		Deflection	
Deviation between min and mean	Deviation between max and mean	Deviation between min and mean	Deviation between max and mean
13.8%	13.7%	7.28%	7.06%

indicates the proportion of the output variability accounted for by the model. Values of R^2 close to 1.0 imply that most of the variability of the output is accounted for by the model while smaller values suggest that the model does not successfully capture variations of the response.

To assess the importance of the input factor \hat{x}_{j_0} we define the new model

$$\tilde{y}_{\text{model}, j_0} = b_0 + \sum_{j=1, j \neq j_0}^m b_j \hat{x}_j \quad (11)$$

and find the set of optimal parameters $\{\tilde{b}_j\}_{j=1, \dots, j_0-1, j_0+1, \dots, m}$ by minimizing the error. The sum of squares (SS) associated with \hat{x}_{j_0} and defined by

$$SS_{j_0} = \sum_{i=1}^n (y_{\text{model}}^{(i)} - \bar{y})^2 - \sum_{i=1}^n (\tilde{y}_{\text{model}, j_0}^{(i)} - \bar{y})^2 \quad (12)$$

measures the importance of the j_0 th input factor.

In order to determine whether coefficients \mathbf{b} appear to be zero or not we use Student's t -test with 5% threshold to reject the zero hypothesis. That is, it is assumed that a term of \mathbf{b} is significant/non-zero if the hypothesis that its actual value be zero has less than 5% probability. Even though the distributional assumptions that lead to the p -values of Student's t -test are not satisfied in sampling-based sensitivity studies these p -values still provide a useful criterion for assessing the importance of a variable (Saltelli et al. [18]).

Results of the sensitivity analysis for the crack length are given in Table 6 for 30% variation in values of all input factors. We have listed in the Table only the significant input factors (less than 5% chance of being zero). Detailed analyses of the variance are provided in the Appendix. Similar results were obtained for 10% variation in the values of the input variables (the five inputs with the most effect are the same, with comparable relative weight and normalized sensitivity coefficients). The sensitivity coefficients were normalized with the largest magnitude of the coefficients that

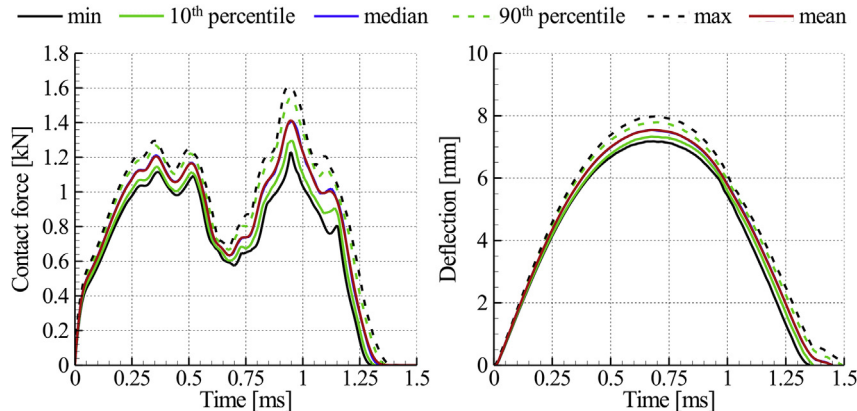


Fig. 11. Histories of the minimum, 10th percentile, 50th and 90th percentiles and mean of the contact force and deflection.

preserves their signs. Thus a positive value of the coefficient indicates that an increase in the input factors induces an increase in the output while it is the opposite for a negative value of the coefficient. We can conclude from results listed in Table 6 that the cumulated SS corresponding to the five elastic moduli of the plate materials accounts for more than 99% of the variability of the output. The factor with the largest coefficient is Young's modulus E for the PMMA. The coefficient is positive meaning that an increase of E induces an increase of the crack length. This is because the threshold stress for the brittle failure was kept constant in the study, meaning that with an increase of E the strain at failure decreases. We also note that the sensitivity coefficient of G_0 is negative, meaning that a softer interlayer will result in longer cracks in the PMMA. This agrees with the experimental results of Stenzler [15] for the softer IM800A interlayer and with the results computed by Antoine and Batra [4] for this interlayer material.

A similar investigation has been carried out for the total energy dissipation and results for 10% and 30% variation of the input factors are summarized in Table 7 and Table 8 where only significant factors are listed. The main source of energy dissipation is plastic deformations of the PC. Thus it is not surprising to find three material parameters of the PC among the five most important parameters for 10% and 30% variation in values of input parameters. In particular two of these parameters are related to its plastic deformations. The three parameters of the PC are Young's modulus, the activation energy of phase α , ΔG_α (plastic yielding), and the softening parameter t_α^{ss} (plastic softening). The two remaining parameters among the five most important ones are Young's modulus of the PMMA and the shear modulus of the interlayer. The signs of the sensitivity coefficients of these five parameters are the same for the two amplitudes of variation, however, Young's modulus of the PMMA is at the second place for the 10% variation study and at the fourth place for the 30% variation study while the remaining parameters have the same relative rankings. In both cases the cumulated SS of these five parameters represents more than 94% of the total SS. Finally we note that the R^2 of the fits of the energy dissipation is smaller than that of the crack length. This may be due to the fact that for the crack length one parameter (E of the PMMA) is clearly dominant while for the energy dissipation many parameters have similar SS, which indicates that more interactions (not accounted for by the linear model of Eq. (8)) are present.

The correlation between the energy dissipation and the crack length cannot be established when the elastic moduli of the PMMA and the PC are fixed since regression analyses yield their correlation to be insignificant. However, when all parameters vary a significant correlation exists. Thus the crack length and the dissipation seem to be correlated via the elastic moduli of the PMMA and the PC.

In order to investigate the reaction force time history we introduce scalar quantities which characterize it. Three noticeable features of the reaction force time history are the first peak, the subsequent minimum value of the force (called "valley" in the following), and the second peak of the force (see Fig. 8). We define

Table 6
Summary of the six parameters with the most influence on the variability of the crack length in the PMMA for the impact of the laminate with 30% variation in values of all input factors. $R^2 = 0.83$.

Material	Parameter	% Total SS	Normalized sensitivity coefficient
PMMA	E	70.9	1.0
PC	E	12.2	-0.41
Adhesive	G_0	9.45	-0.37
PC	ν	3.57	-0.23
PMMA	ν	2.91	0.20
PC	ΔG_β	0.66	-0.096
Total		99.7	

Table 7
Parameters with the most influence on the output variability of the energy dissipation for the impact problem with 10% variation in all input factors $R^2 = 0.63$.

Material	Parameter	% Total SS	Normalized sensitivity coefficient
PC	E	31.4	-1.0
PMMA	E	25.6	0.91
PC	ΔG_α	20.7	-0.81
PC	t_α^{ss}	10.7	-0.59
Adhesive	G_0	5.90	0.44
PC	ΔG_β	3.79	0.35
PMMA	ν	1.64	0.23
Total		99.7	

Table 8
Parameters with the most influence on the output variability of the energy dissipation for the study with 30% variation in all input factors, $R^2 = 0.78$.

Material	Parameter	% Total SS	Normalized sensitivity coefficient
PC	E	39.5	-1.0
PC	ΔG_α	21.3	-0.73
PC	t_α^{ss}	13.7	-0.59
PMMA	E	12.6	0.57
Adhesive	G_0	9.24	0.49
PMMA	ν	2.18	0.24
PMMA	ΔG_α	1.05	-0.16
Total		99.6	

the first peak of the reaction force as its local maximum between 0.0 and 0.65 ms, the second peak as its local maximum between 0.75 and 1.6 ms, and the valley value as its local minimum between times 0.5 and 0.9 ms.

Linear models of the form of Eq. (8) including all input factors could be fitted to accurately capture the 1st peak and the valley of the reaction forces ($R^2 > 0.95$, see values in the left column of Table 9). Thus the magnitudes of the 1st peak and the valley in the reaction force can be expressed as linear functions of the material parameters. Moreover, when the elastic moduli of the PC and the PMMA are varied, E and ν of the PMMA and the PC and G_0 of the adhesive account for more than 85% of the variability of the model (their cumulated partial SS is larger than 85% of the total SS) for the 1st peak and the valley.

A satisfactory linear model giving the amplitude of the 2nd peak as an affine function of the input factors cannot be found since R^2 -values of 0.62 and 0.59 were obtained for 10% and 30% variations of the inputs, respectively (see Table 9, left column). Upon studying the correlation Tables given in the Appendix we notice that the 2nd peak of the reaction force time history is strongly correlated with the energy dissipated. In order to investigate this correlation, a simple model expressing the 1st peak, the valley and the 2nd peak as linear functions of the energy dissipation only are fitted to the numerical results. The corresponding R^2 -values are listed in Table 9.

The correlation between the 2nd peak in the reaction force time history and the energy dissipation is clear since expressing the

Table 9
Values of R^2 for the reaction force as a function of either the material parameters or the energy dissipation alone.

Case	Variables as function of all material parameters			Variables as function of the dissipation only		
	1st peak	valley	2nd peak	1st peak	valley	2nd peak
All inputs $\pm 10\%$	0.986	0.990	0.624	0.019	0.088	0.756
All inputs $\pm 30\%$	0.957	0.983	0.593	0.107	0.081	0.686
Fixed E and ν for PMMA and PC, other inputs $\pm 10\%$	0.955	0.934	0.529	0.042	0.014	0.511
Fixed E and ν for PMMA and PC, -other inputs $\pm 30\%$	0.873	0.943	0.640	0.345	0.239	0.627

value of the 2nd peak as an affine function of the energy dissipated gives $R^2 = \sim 0.7$ in the first two cases as compared to R^2 between 0.5 and 0.6 with fixed values of E for the PMMA and the PC. To visualize this correlation the 2nd peak of the contact force is plotted as a function of the energy dissipated in Fig. 12.

The affine fits in Fig. 12 have negative slopes meaning that the energy dissipated and the 2nd peak of the contact force have opposite variations. This implies that when the plate dissipates more energy it has less elastic energy to bounce back. Thus the contact force corresponding to the rebound of the impactor (2nd peak of the reaction force, see Ref. [4]) has smaller magnitude.

One could argue that since the energy dissipation and the elastic properties of the PMMA and the PC are correlated, a correlation between the 2nd peak in the reaction force time history and the energy dissipated may simply mean that the 2nd peak is correlated with the elastic properties of these materials. This can be refuted by observing that the correlation between the dissipation and the 2nd peak of the reaction force still holds when the elastic properties of the PMMA and the PC materials are fixed at their nominal values (see the two last rows of Table 9).

The slopes of the affine fits of Fig. 12 are given in Table 10. We note that the coefficients are similar for all cases suggesting that the underlying mechanisms that correlate the 2nd peak of the reaction force and the energy dissipated are identical whether or not the elastic properties of the PMMA and the PC are varied.

For variations in values of the geometric parameters and the impact speed, results of the sensitivity study of the dissipation and of the crack length are summarized in Tables 11 and 12, respectively. For the dissipation all parameters except the thickness of the PC are significant (with 95% confidence). For the crack length the thickness of the PC plate and the impact speed are significant but the thickness of the PMMA plate and of the adhesive have negligible effect.

5. Conclusions

For the polymethylmethacrylate (PMMA) and the polycarbonate (PC) we have identified material parameters that significantly affect their stress-strain response in uniaxial compression. Those and other parameters have been used to perform sensitivity analyses of the low velocity impact by a rigid impactor of a laminated PMMA/DFA4700 adhesive/PC plate. The variations in the shear modulus of the DFA4700 interlayer have also been considered in the sensitivity study.

The effect of uncertainties in values of material parameters on variations in the response of the laminated plate has been investigated. It has been found that the elastic properties of the

Table 10

Regression coefficients of energy dissipated for the 2nd peak of the reaction force as an affine function of the energy dissipated.

	Regression coefficient (kN/J)
All inputs $\pm 10\%$	-0.490
All inputs $\pm 30\%$	-0.380
Fixed E and ν for PMMA and PC, other inputs $\pm 10\%$	-0.335
Fixed E and ν for PMMA and PC, other inputs $\pm 30\%$	-0.396

Table 11

Summary of the dissipation variability, $R^2 = 0.88$.

Parameter	% Total SS	Sensitivity coefficient
Thickness of PMMA	34.4	-2.17 J/mm
Thickness of adhesive	13.3	-1.35 J/mm
Thickness of PC	0.54	-0.271 J/mm
Impact velocity	51.8	0.203 J/(m/s)
Total	100	

Table 12

Summary of the crack length variability, $R^2 = 0.71$.

Parameter	% Total SS	Sensitivity coefficient
Thickness of PMMA	0.00	-0.039 mm/mm
Thickness of adhesive	1.37	0.785 mm/mm
Thickness of PC	36.2	-4.03 mm/mm
Impact velocity	62.43	0.403 mm/(m/s)
Total	100.0	

constituents of the plate dominantly affect the plate response, which is good since they can be easily measured experimentally. However, the energy dissipated is mostly affected by parameters that affect the plastic yielding and the plastic softening of the PC, which is consistent with the previously reported result that the energy dissipated is mostly due to plastic deformations of the PC. Thus even when the experimentally measurable quantities such as the plate deflection, the crack length and the reaction force agree with their corresponding experimental values and have very little variability due to the uncertainty in the values of material parameters, the scatter in the energy dissipation may be considerable. This indicates that even if a mathematical model has been validated by establishing a close agreement between its predictions of plate deflections etc. with the experimental results the computed energy dissipated may be far from that actually dissipated in the plate. Interactions among different material parameters could explain this larger scatter in the energy dissipated.

We found that the 1st peak and the valley but not the 2nd peak in the reaction force time history can be accurately expressed as

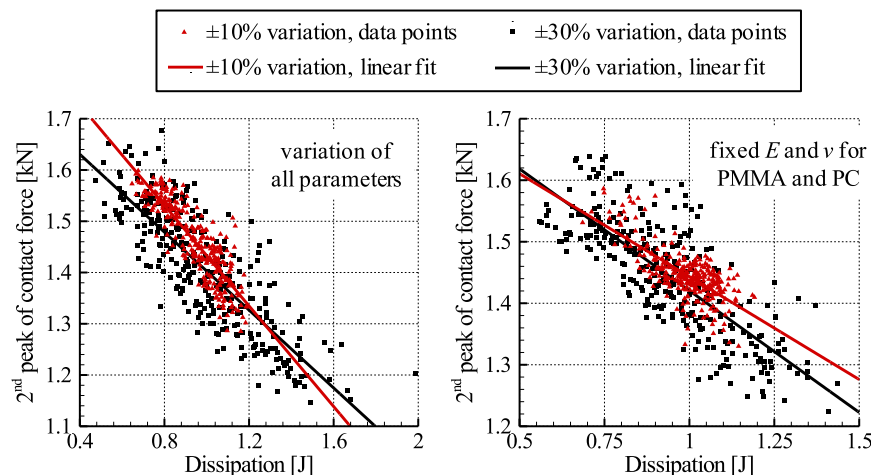


Fig. 12. Value of the 2nd peak of the reaction force as a function of the energy dissipation and affine fit for all cases studied.

functions of material parameters of the constituents of the plate. The 2nd peak in the reaction force time history is correlated with the energy dissipated in the plate. It suggests that capturing the amplitude of the 2nd peak of the reaction force history requires that the mathematical model of the problem accurately predict the energy dissipated during the impact event.

Acknowledgments

This research was sponsored by the US Army Research Laboratory and was accomplished under Cooperative Agreement Number W911NF-06-2-0014. The views and conclusions contained in this

document are those of the authors and should not be interpreted as representing the official policies, either expressed or implied, of the Army Research Laboratory or the U.S. Government. The U.S. Government is authorized to reproduce and distribute reprints for Government purposes notwithstanding any copyright notation hereon.

Appendix

A1. Variations in the material parameters

Correlation of the inputs and the outputs

	x1	x2	x3	x4	x5	x6	x7	x8	x9	x10	x11	y1	y2	y3	y4	y5
(a)	1.000	1.000														
	-0.021	-0.035														
	0.084	0.023	1.000													
	0.056	-0.054	-0.055	1.000												
	0.011	-0.021	0.008	-0.022	0.003	1.000										
	-0.018	0.033	-0.070	-0.054	0.000	-0.063	1.000									
	-0.021	0.008	-0.019	-0.002	0.030	-0.029	-0.004	1.000								
	-0.014	-0.022	-0.061	0.059	-0.007	0.029	-0.043	0.001	1.000							
	-0.001	0.010	-0.032	-0.026	-0.060	-0.001	0.022	0.013	-0.043	1.000						
	0.036	0.049	0.035	0.071	-0.044	-0.027	-0.033	0.007	0.089	-0.017	1.000					
	0.410	0.116	0.030	0.067	-0.029	-0.441	0.040	-0.348	-0.269	0.157	0.198	1.000				
	0.751	0.059	-0.005	0.098	0.044	-0.273	-0.102	-0.083	-0.093	-0.048	-0.251	0.551	1.000			
	0.516	0.045	-0.042	0.000	0.031	0.693	0.292	0.154	0.110	0.281	0.039	-0.138	0.086	1.000		
	0.710	0.564	-0.047	0.072	0.008	0.185	0.194	-0.065	-0.036	-0.139	0.262	0.297	0.431	0.556	1.000	
	-0.528	-0.136	0.008	-0.051	0.013	0.460	0.014	0.257	0.205	0.063	-0.018	-0.869	-0.682	0.152	-0.361	1.000
(b)	1.000	1.000														
	-0.021	-0.035														
	0.084	0.023	1.000													
	0.056	-0.054	-0.055	1.000												
	0.011	-0.021	0.008	-0.022	0.003	1.000										
	-0.018	0.033	-0.070	-0.054	0.000	-0.063	1.000									
	-0.021	0.008	-0.019	-0.002	0.030	-0.029	-0.004	1.000								
	-0.014	-0.022	-0.061	0.059	-0.007	0.029	-0.043	0.001	1.000							
	-0.001	0.010	-0.032	-0.026	-0.060	-0.001	0.022	0.013	-0.043	1.000						
	0.036	0.049	0.035	0.071	-0.044	-0.027	-0.033	0.007	0.089	-0.017	1.000					
	0.410	0.116	0.030	0.067	-0.029	-0.441	0.040	-0.348	-0.269	0.157	0.198	1.000				
	0.751	0.059	-0.005	0.098	0.044	-0.273	-0.102	-0.083	-0.093	-0.048	-0.251	0.551	1.000			
	0.516	0.045	-0.042	0.000	0.031	0.693	0.292	0.154	0.110	0.281	0.039	-0.138	0.086	1.000		
	0.710	0.564	-0.047	0.072	0.008	0.185	0.194	-0.065	-0.036	-0.139	0.262	0.297	0.431	0.556	1.000	
	-0.528	-0.136	0.008	-0.051	0.013	0.460	0.014	0.257	0.205	0.063	-0.018	-0.869	-0.682	0.152	-0.361	1.000
	1.000	1.000														
	-0.021	-0.035														
	0.084	0.023	1.000													
	0.056	-0.054	-0.055	1.000												
	0.011	-0.021	0.008	-0.022	0.003	1.000										
	-0.018	0.033	-0.070	-0.054	0.000	-0.063	1.000									
	-0.021	0.008	-0.019	-0.002	0.030	-0.029	-0.004	1.000								
	-0.014	-0.022	-0.061	0.059	-0.007	0.029	-0.043	0.001	1.000							
	-0.001	0.010	-0.032	-0.026	-0.060	-0.001	0.022	0.013	-0.043	1.000						
	0.036	0.049	0.035	0.071	-0.044	-0.027	-0.033	0.007	0.089	-0.017	1.000					
	0.410	0.116	0.030	0.067	-0.029	-0.441	0.040	-0.348	-0.269	0.157	0.198	1.000				
	0.751	0.059	-0.005	0.098	0.044	-0.273	-0.102	-0.083	-0.093	-0.048	-0.251	0.551	1.000			
	0.516	0.045	-0.042	0.000	0.031	0.693	0.292	0.154	0.110	0.281	0.039	-0.138	0.086	1.000		
	0.710	0.564	-0.047	0.072	0.008	0.185	0.194	-0.065	-0.036	-0.139	0.262	0.297	0.431	0.556	1.000	
	-0.528	-0.136	0.008	-0.051	0.013	0.460	0.014	0.257	0.205	0.063	-0.018	-0.869	-0.682	0.152	-0.361	1.000
	1.000	1.000														
	-0.021	-0.035														
	0.084	0.023	1.000													
	0.056	-0.054	-0.055	1.000												
	0.011	-0.021	0.008	-0.022	0.003	1.000										
	-0.018	0.033	-0.070	-0.054	0.000	-0.063	1.000									
	-0.021	0.008	-0.019	-0.002	0.030	-0.029	-0.004	1.000								
	-0.014	-0.022	-0.061	0.059	-0.007	0.029	-0.043	0.001	1.000							
	-0.001	0.010	-0.032	-0.026	-0.060	-0.001	0.022	0.013	-0.043	1.000						
	0.036	0.049	0.035	0.071	-0.044	-0.027	-0.033	0.007	0.089	-0.017	1.000					
	0.410	0.116	0.030	0.067	-0.029	-0.441	0.040	-0.348	-0.269	0.157	0.198	1.000				
	0.751	0.059	-0.005	0.098	0.044	-0.273	-0.102	-0.083	-0.093	-0.048	-0.251	0.551	1.000			
	0.516	0.045	-0.042	0.000	0.031	0.693	0.292	0.154	0.110	0.281	0.039	-0.138	0.086	1.000		
	0.710	0.564	-0.047	0.072	0.008	0.185	0.194	-0.065	-0.036	-0.139	0.262	0.297	0.431	0.556	1.000	
	-0.528	-0.136	0.008	-0.051	0.013	0.460	0.014	0.257	0.205	0.063	-0.018	-0.869	-0.682	0.152	-0.361	1.000
	1.000	1.000														
	-0.021	-0.035														
	0.084	0.023	1.000													
	0.056	-0.054	-0.055	1.000												
	0.011	-0.021	0.008	-0.022	0.003	1.000										
	-0.018	0.033	-0.070	-0.054	0.000	-0.063	1.000									
	-0.021	0.008	-0.019	-0.002	0.030	-0.029	-0.004	1.000								
	-0.014	-0.022	-0.061	0.059	-0.007	0.029	-0.043	0.001	1.000							
	-0.001	0.010	-0.032	-0.026	-0.060	-0.001	0.022	0.013	-0.043	1.000						
	0.036	0.049	0.035	0.071	-0.044	-0.027	-0.033	0.007	0.089	-0.017	1.000					
	0.410	0.116	0.030	0.067	-0.029	-0.441	0.040	-0.348	-0.269	0.157	0.198	1.000				
	0.751	0.059	-0.005	0.098	0.044	-0.273	-0.102	-0.083	-0.093	-0.048	-0.251	0.551	1.000			
	0.516	0.045	-0.042	0.000	0.031	0.693	0.292	0.154	0.110	0.281	0.039	-0.138	0.086	1.000		
	0.710	0.564	-0.047	0.072	0.008	0.185	0.194	-0.065	-0.036	-0.139	0.262	0.297	0.431	0.556	1.000	
	-0.528	-0.136	0.008	-0.051	0.013	0.460	0.014	0.257	0.205	0.063	-0.018	-0.869	-0.682	0.152	-0.361	1.000
	1.000	1.000														
	-0.021	-0.035														
	0.084	0.023	1.000													
	0.056	-0.054	-0.055	1.000												
	0.011	-0.021	0.008	-0.022	0.003	1.000										
	-0.018	0.033	-0.070	-0.054	0.000	-0.063	1.000									
	-0.021	0.008	-0.019	-0.002	0.030	-0.029	-0.004	1.00								

Table 17
Normalized sensitivity coefficients, *p*- and *R*² values for ±30% variation of all input factors.

Input factor	Dissipation		Crack length		
	Normalized sensitivity coefficient	<i>p</i> -value	Normalized sensitivity coefficient	<i>p</i> -value	
PMMA	<i>E</i>	0.565	<0.0001	1.00	<0.0001
	<i>ν</i>	0.235	<0.0001	0.202	<0.0001
	ΔG_α	-0.164	0.001	-0.022	0.487
	α_β^p	-0.057	0.264	0.006	0.837
PC	t_β^{ss}	-0.055	0.274	-0.014	0.651
	<i>E</i>	-1.00	<0.0001	-0.413	<0.0001
	<i>ν</i>	-0.041	0.412	-0.225	<0.0001
	ΔG_α	-0.733	<0.0001	-0.028	0.374
	t_α^{ss}	-0.592	<0.0001	-0.058	0.062
Adhesive	ΔG_β	-0.058	0.245	-0.096	0.0022
	<i>G</i> ₀	0.486	<0.0001	-0.366	<0.0001
<i>R</i> ²	0.778		0.831		

Table 18
ANOVA for the dissipation for ±30% variation of all input factors.

Material	Parameter	Sum of squares (SS)	% Total SS	DOF	Mean SS	F
PC	<i>E</i>	6.005	39.52	1	6.005	397.1
PC	ΔG_α	3.239	21.32	1	3.239	214.2
PC	t_α^{ss}	2.082	13.7	1	2.082	137.7
PMMA	<i>E</i>	1.907	12.55	1	1.907	126.1
Adhesive	<i>G</i> ₀	1.403	9.24	1	1.403	92.8
PMMA	<i>ν</i>	0.332	2.18	1	0.332	21.93
PMMA	ΔG_α	0.159	1.05	1	0.159	10.51
PC	ΔG_β	0.021	0.13	1	0.021	
PMMA	α_β^p	0.019	0.12	1	0.019	
PMMA	t_β^{ss}	0.018	0.12	1	0.018	
PC	<i>ν</i>	0.01	0.07	1	0.01	
Total		15.19	100			

Table 19
ANOVA for the crack length for ±30% variation of all input factors.

Material	Parameter	Sum of squares (SS)	% Total SS	DOF	Mean SS	F
PMMA	<i>E</i>	2251.	70.89	1	2251.	1034.
PC	<i>E</i>	386.7	12.17	1	386.7	177.5
Adhesive	<i>G</i> ₀	300.3	9.45	1	300.3	137.9
PC	<i>ν</i>	113.5	3.57	1	113.5	52.12
PMMA	<i>ν</i>	92.38	2.91	1	92.38	42.41
PC	ΔG_β	20.83	0.66	1	20.83	9.56
PC	t_α^{ss}	7.650	0.24	1	7.650	
PC	ΔG_α	1.726	0.05	1	1.726	
PMMA	ΔG_α	1.054	0.03	1	1.054	
PMMA	t_β^{ss}	0.446	0.01	1	0.446	
PMMA	α_β^p	0.093	0	1	0.093	
Total		3176.3	100			

Table 20
Normalized sensitivity coefficients, *p*- and *R*² values for ±10% variation of all input factors except for Young's moduli and Poisson's ratios of PMMA and PC.

Input factor	Dissipation		Crack length		
	Normalized sensitivity coefficient	<i>p</i> -value	Normalized sensitivity coefficient	<i>p</i> -value	
PMMA	<i>E</i>	N/A	N/A		
	<i>ν</i>				
	ΔG_α	0.549	<0.0001	0.616	<0.0001
	α_β^p	0.040	0.615	0.063	0.482
PC	t_β^{ss}	0.013	0.867	-0.026	0.769
	<i>E</i>	N/A		N/A	
	<i>ν</i>				
	ΔG_α	-1.0	<0.0001	-0.235	0.009
	t_α^{ss}	-0.628	<0.0001	-0.016	0.861
Adhesive	ΔG_β	0.300	0.0002	0.014	0.880
	<i>G</i> ₀	0.475	<0.0001	-1.00	<0.0001
<i>R</i> ²	0.52		0.38		

Table 21
ANOVA for the dissipation for ±10% variation of all input factors except the elastic moduli of PMMA and PC.

Material	Parameter	Sum of squares (SS)	% Total SS	DOF	Mean SS	F
PC	ΔG_α	0.572	49.98	1	0.572	157.36
PC	t_α^{ss}	0.222	19.43	1	0.222	61.17
PMMA	ΔG_α	0.171	14.91	1	0.171	46.94
Adhesive	<i>G</i> ₀	0.127	11.12	1	0.127	35.00
PC	ΔG_β	0.051	4.48	1	0.051	14.11
PMMA	α_β^p	0.001	0.08	1	0.001	
PMMA	t_β^{ss}	0.0001	0.01	1	0.0001	
Total		1.145	100			

Table 22
ANOVA for the crack length for ±10% variation of all input factors except for the elastic moduli of PMMA and PC.

Material	Parameter	Sum of squares (SS)	% Total SS	DOF	Mean SS	F
Adhesive	<i>G</i> ₀	5.569	69.35	1	5.569	124.77
PMMA	ΔG_α	2.122	26.42	1	2.122	47.53
PC	ΔG_α	0.311	3.88	1	0.311	6.97
PMMA	α_β^p	0.022	0.28	1	0.022	
PMMA	t_β^{ss}	0.004	0.05	1	0.004	
PC	t_α^{ss}	0.001	0.02	1	0.001	
PC	ΔG_β	0.001	0.01	1	0.001	
Total		8.03	100			

Table 23
Normalized sensitivity coefficients, *p*- and *R*² values for ±30% variation of all input factors except for Young's moduli and Poisson's ratios of PMMA and PC.

Input factor	Dissipation		Crack length		
	Normalized sensitivity coefficient	<i>p</i> -value	Normalized sensitivity coefficient	<i>p</i> -value	
PMMA	<i>E</i>	N/A	N/A		
	<i>ν</i>				
	ΔG_α	0.343	<0.0001	0.132	0.001
	α_β^p	-0.015	0.725	-0.037	0.328
PC	t_β^{ss}	-0.022	0.606	-0.022	0.558
	<i>E</i>	N/A		N/A	
	<i>ν</i>				
	ΔG_α	-1.0	<0.0001	-0.112	0.003
	t_α^{ss}	-0.702	<0.0001	-0.104	0.006
Adhesive	ΔG_β	-0.083	0.051	-0.228	<0.0001
	<i>G</i> ₀	0.511	<0.0001	-1.0	<0.0001
<i>R</i> ²	0.784		0.732		

Table 24

ANOVA for the dissipation for ±30% variation of all input factors except for the elastic moduli of PMMA and PC.

Material	Parameter	Sum of squares (SS)	% Total SS	DOF	Mean SS	F
PC	ΔG_α	4.203	53.53	1	4.203	565.79
PC	t_α^{SS}	2.041	26	1	2.041	274.73
Adhesive	G_0	1.084	13.81	1	1.084	145.97
PMMA	ΔG_α	0.491	6.26	1	0.491	66.15
PC	ΔG_β	0.028	0.36	1	0.028	
PMMA	t_β^{SS}	0.002	0.03	1	0.002	
PMMA	α_β^p	0.001	0.01	1	0.001	
Total		7.85	100			

Table 25

ANOVA for the crack length for ±30% variation of all input factors except for the elastic moduli of PMMA and PC.

Material	Parameter	Sum of squares (SS)	% Total SS	DOF	Mean SS	F
Adhesive	G_0	159.1	91.31	1	159.1	713.27
PC	ΔG_β	8.345	4.79	1	8.345	37.42
PMMA	ΔG_α	2.762	1.59	1	2.762	12.38
PC	ΔG_α	2.007	1.15	1	2.007	9
PC	t_α^{SS}	1.728	0.99	1	1.728	7.75
PMMA	α_β^p	0.214	0.12	1	0.214	
PMMA	t_β^{SS}	0.077	0.04	1	0.077	
Total		174.2	100			

A2. Variations in the layer thicknesses and in the impact velocity

Correlation of the inputs and the outputs

x1	1.000								
x2	0.053	1.000							
x3	-0.004	0.048	1.000						
x4	-0.053	0.041	-0.012	1.000					
y1	-0.589	-0.338	-0.088	0.674	1.000				
y2	-0.033	0.101	-0.507	0.673	0.561	1.000			
y3	0.179	0.137	0.168	0.953	0.476	0.559	1.000		
y4	-0.108	-0.343	-0.288	0.882	0.761	0.681	0.747	1.000	
y5	0.855	0.093	0.165	-0.013	-0.637	-0.161	0.218	-0.126	1.000
	x1	x2	x3	x4	y1	y2	y3	y4	y5

key to the inputs and outputs

x1: thickness of PMMA	x4: impact velocity v_0	y3: reforc, 1 st peak
x2: thickness of adhesive	y1: dissipation	y4: reforc, valley
x3: thickness of PC	y2: crack length	y5: reforc, 2 nd peak

Fig. 13. Histories of minimum, 10th percentile, 50th and 90th percentiles and mean of the contact force and deflection.

ANOVA.

Table 26

ANOVA for the dissipation for variations in the layer thicknesses and in the impact velocity.

Parameter	Sum of squares (SS)	% Total SS	DOF	Mean SS	F
Impact velocity	1.367	51.78	1	1.367	338.66
Thickness of PMMA	0.908	34.4	1	0.908	224.99
Thickness of adhesive	0.351	13.29	1	0.351	86.9
Thickness of PC	0.014	0.54	1	0.014	
Total	2.64	100			

Table 27

ANOVA for the crack length for variations in the layer thicknesses and in the impact velocity.

Parameter	Sum of Squares (SS)	% total SS	DOF	Mean SS	F
Impact velocity	5.404	62.43	1	5.404	143.87
Thickness of PC	3.133	36.2	1	3.133	83.42
Thickness of adhesive	0.118	1.37	1	0.118	
Thickness of PMMA	0.00	0.00	1	0.00	
Total	8.655	100			

A3. Material model for the transparent material

The material models for the PMMA and the PC differ only in the values of material parameters. We thus briefly describe material model for the PC, and refer the reader to Mulliken and Boyce [5] and Varghese and Batra [6] for details. We assume that the total Cauchy stress tensor σ at a material point equals the sum of contributions from three phases, namely B, α and β , i.e., $\sigma = \sigma_B + \sigma_\alpha + \sigma_\beta$. The three phases coexist at a material point and have the same value of the deformation gradient \mathbf{F} . The phase B behaves like a non-linear elastic Langevin spring for which

$$\sigma_B = \frac{C_R}{3} \frac{\sqrt{N_I}}{\lambda^p} L^{-1} \left(\frac{\lambda^p}{\sqrt{N_I}} \right) \bar{\mathbf{B}}'_B \quad (13)$$

Here σ_B is the Cauchy stress tensor, $\bar{\mathbf{B}}'_B$ the deviatoric part of $\bar{\mathbf{B}}_B = (J)^{-2/3} \mathbf{F} \mathbf{F}^T$, $\lambda^p = \sqrt{\text{tr}(\bar{\mathbf{B}}_B)}/3$ a measure of stretch, $\text{tr}()$ the trace operator, \mathbf{F} the deformation gradient, J the determinant of \mathbf{F} , L^{-1} the inverse of the Langevin function defined by $L(\beta) \equiv \coth \beta - 1/\beta$, N_I

the limiting stretch, $C_R \equiv n_R k \theta$ the rubbery modulus, θ the temperature in Kelvin, k Boltzmann's constant, and n_R a material parameter.

The other two phases, α and β , are modeled with the same constitutive equation but with different values of material parameters. For each phase the deformation gradient \mathbf{F} is decomposed into elastic and plastic parts, $\mathbf{F} = \mathbf{F}_\alpha^e \mathbf{F}_\alpha^p = \mathbf{F}_\beta^e \mathbf{F}_\beta^p$. The rate of the plastic deformation gradient, $\dot{\mathbf{F}}_\alpha^p$, in phases α and β is given by

$$\mathbf{F}_\alpha^p = \mathbf{F}_\alpha^{e-1} \mathbf{D}_\alpha^p \mathbf{F}_\alpha, \quad \mathbf{F}_\beta^p = \mathbf{F}_\beta^{e-1} \mathbf{D}_\beta^p \mathbf{F}_\beta \quad (14)$$

where \mathbf{D}_i^p is the plastic strain rate tensor in phase i ($i = \alpha, \beta$), and it has been assumed that the plastic spin tensors in phases α and β identically vanish.

The Hencky elastic strain tensors of phases α and β are defined as

$$\mathbf{e}_\alpha^e = \ln(\sqrt{\mathbf{F}_\alpha^e \mathbf{F}_\alpha^{eT}}), \quad \mathbf{e}_\beta^e = \ln(\sqrt{\mathbf{F}_\beta^e \mathbf{F}_\beta^{eT}}) \quad (15)$$

and the corresponding Cauchy stress tensors are given by

$$\boldsymbol{\sigma}_\alpha = \frac{1}{J} [2\mu_\alpha \mathbf{e}_\alpha^e + \lambda_\alpha \text{tr}(\mathbf{e}_\alpha^e) \boldsymbol{\delta}], \quad \boldsymbol{\sigma}_\beta = \frac{1}{J} [2\mu_\beta \mathbf{e}_\beta^e + \lambda_\beta \text{tr}(\mathbf{e}_\beta^e) \boldsymbol{\delta}] \quad (16)$$

where Young's moduli of phases α and β of the PC and consequently Lamé's constants, λ and μ , are temperature and strain-rate dependent. We note that Eq. (16) is valid for finite deformations and accounts for all geometric nonlinearities.

The plastic strain rates, \mathbf{D}_α^p , are assumed to be coaxial with the deviatoric Cauchy stress tensors in their respective phases, that is

$$\mathbf{D}_\alpha^p = \dot{\gamma}_\alpha^p \frac{\boldsymbol{\sigma}'_\alpha}{|\boldsymbol{\sigma}'_\alpha|}, \quad \mathbf{D}_\beta^p = \dot{\gamma}_\beta^p \frac{\boldsymbol{\sigma}'_\beta}{|\boldsymbol{\sigma}'_\beta|} \quad (17)$$

where $\boldsymbol{\sigma}'_i$ ($i = \alpha, \beta$) is the deviatoric part of the Cauchy stress in phase i , $|\boldsymbol{\sigma}'_i| = \sqrt{\text{tr}(\boldsymbol{\sigma}'_i \boldsymbol{\sigma}'_i)}$ is the magnitude of $\boldsymbol{\sigma}'_i$, and $\dot{\gamma}_i^p$ is the effective plastic strain rate in phase i . This equation implies that $\text{tr}(\mathbf{D}_i^p) = 0$.

The effective plastic strain rates in α and β phases are given by

$$\dot{\gamma}_i^p = \dot{\gamma}_{0i}^p \exp \left[-\frac{\Delta G_i}{k\theta} \left(1 - \frac{\tau_i}{t_i \hat{s}_i + \alpha_i^p p} \right) \right], \quad i = \alpha, \beta \quad (18)$$

where $\dot{\gamma}_{0i}^p$ ($i = \alpha, \beta$) is the pre-exponential factor, ΔG_i the activation energy, $p = -\text{tr}(\boldsymbol{\sigma})/3$ the pressure, $\tau_i = \sqrt{0.5 \text{tr}(\boldsymbol{\sigma}'_i \boldsymbol{\sigma}'_i)}$ the effective stress, α_i^p the pressure coefficient, $\hat{s}_i = 0.077 \mu_i / (1 - \nu_i)$ the athermal shear strength, ν_i Poisson's ratio, k Boltzmann's constant, and t_i an internal variable that evolves with plastic deformations. The evolution of internal variable t_i in phases α and β is given by

$$\dot{t}_i = \frac{h_i}{\hat{s}_i^0} \left(1 - \frac{t_i}{t_i^{ss}} \right) \dot{\gamma}_i^p, \quad i = \alpha, \beta \quad (19)$$

where t_i^{ss} and h_i are softening parameters, and \hat{s}_i^0 is the reference value of \hat{s}_i given by the reference values of μ_i and ν_i .

We postulate that the energy dissipated during plastic deformations in the α and β phases is converted into heat, that is

$$\dot{Q} = J \left(\boldsymbol{\sigma}_\alpha : \mathbf{D}_\alpha^p + \boldsymbol{\sigma}_\beta : \mathbf{D}_\beta^p \right) \quad (20)$$

where \dot{Q} is the heat generated per unit volume in the reference configuration.

We refer the reader to Mulliken's thesis [7], Mulliken and Boyce [5] and Varghese and Batra [6] for the determination of values of the 16 material parameters from the test data for the PC that are given in Table 28, and for the comparison of the computed and experimental axial stress vs. axial strain curves.

Table 28

Nominal values of material parameters for the PC.

	Phase α	Phase β	Phase B	Common
ν_i	0.38	0.38		
$\dot{\gamma}_{0i}^p$ [/s]	2.94×10^{16}	3.39×10^5		
ΔG_i [J]	3.744×10^{-19}	3.769×10^{-20}		
α_i^p	0.168	0.245		
h_i [MPa]	125	400		
t_i^{ss}	0.33	2.00		
C_R at 300 K [MPa]			35.0	
N_i			12.25	
ρ [g/cm ³]				1.20
E [GPa] at 300 K, 5000/s	1.678	0.344		

References

- Anderson CE, Holmquist TJ. Application of a computational glass model to compute propagation of failure from ballistic impact of borosilicate glass targets. *Int J Impact Eng* 2013;56:2–11.
- Anderson Jr CE, Holmquist TJ. Computational modeling of failure for hyper-velocity impacts into glass targets. *Procedia Eng* 2013;58:194–203.
- Poteet CC, Blosser ML. Improving metallic thermal protection system hyper-velocity impact resistance through numerical simulations. *J Space and Rockets* 2004;41:221–31.
- Antoine GO, Batra RC. Low speed impact of laminated polymethylmethacrylate/adhesive/polycarbonate plates. *Compos Struct* 2014;116:193–210.
- Mulliken AD, Boyce MC. Mechanics of the rate-dependent elastic-plastic deformation of glassy polymers from low to high strain rates. *Int J Solids Struct* 2006;43:1331–56.
- Varghese AG, Batra RC. Constitutive equations for thermomechanical deformations of glassy polymers. *Int J Solids Struct* 2009;46:4079–94.
- Mulliken AD. Mechanics of amorphous polymers and polymer nanocomposites during high rate deformation. M.Sc. thesis. Massachusetts: Institute of Technology; 2006. p. 290.
- Fleck NA, Stronge WJ, Liu JH. High strain-rate shear response of polycarbonate and polymethyl methacrylate. *P Roy Soc Lond A Mat* 1990;429:459.
- Stickle AM, Schultz PH. Exploring the role of shear in oblique impacts: a comparison of experimental and numerical results for planar targets. *Int J Impact Eng* 2011;38:527–34.
- Richards M, Clegg R, Howlett S. Ballistic performance assessment of glass laminates through experimental and numerical investigation. In: Reinecke WG, editor. *Proceedings of the 18th international symposium on Ballistics* San Antonio, Texas, USA, 15–19 Nov.1999. Technomic Publishing Company, Inc.; 1999. p. 1123–30.
- Zhang W, Tekalur SA, Huynh L. Impact behavior and dynamic failure of PMMA and PC plates. In: Proulx T, editor. *Dynamic behavior of materials* Indianapolis, Indiana, USA, 7–10 June 2010, vol. 1. Springer; 2011. p. 93–104.
- Gunnarsson CA, Ziemski B, Weerasooriya T, Moy P. Deformation and failure of polycarbonate during impact as a function of thickness. In: *Proceedings of the 2009 international congress and exposition on experimental mechanics and applied mechanics* Albuquerque, New Mexico, USA, 1–4 June 2009. Curran Associates, Inc.; 2009. p. 1500–11.
- Ogden RW. *Non-linear elastic deformations*. Chichester, Great Britain: Ellis Horwood Ltd.; 1984.
- Christensen RM. A non-linear theory of viscoelasticity for application to elastomers. *J Appl Mech-T ASME* 1980;47:762–8.
- Stenzler JS. Impact mechanics of PMMA/PC multi-laminates with soft polymer interlayers. M.Sc. thesis. Blacksburg, VA: University Libraries, Virginia Polytechnic Institute and State University; 2009.
- Stenzler JS, Goulbourne N. Impact mechanics of transparent multi-layered polymer composites. In: *Society for experimental mechanics-sem annual conference and exposition on experimental and applied mechanics* Albuquerque, New Mexico, USA, 1–4 June 2009; 2009. V3.
- Morris MD. Factorial sampling plans for preliminary computational experiments. *Technometrics* 1991;33:161–74.
- Saltelli A, Chan K, Scott EM. *Sensitivity analysis*. New York: Wiley; 2000.
- Iman RL, Helton JC, Campbell JE. An approach to sensitivity analysis of computer-models. 1. Introduction, input variable selection and preliminary variable assessment. *J Qual Technol* 1981;13:174–83.
- Iman RL, Helton JC, Campbell JE. An approach to sensitivity analysis of computer-models. 2. Ranking of input variables, response-surface validation, distribution effect and technique synopsis. *J Qual Technol* 1981;13:232–40.
- Comets F. Introduction aux probabilités et à la simulation aléatoire-polycopié du département de mathématiques appliquées. Ecole Polytechnique-Edition; 2004.
- Antoine GO, Batra RC. Constitutive relations and parameter estimation for finite deformations of viscoelastic adhesives. *ASME – J Appl Mechs* 2015;82. Art. No. 021001.